Bulletin of Electrical Engineering and Informatics
Vol. 15, No. 1, February 2026, pp. 845~859
ISSN: 2302-9285, DOI: 10.11591/eei.v15i1.10531

Delineating 12-lead ECG for automated ST-elevation and ST-depression detection using deep learning

Bambang Tutuko[1,2], Annisa Darmawahyuni[1,2], Alexander Edo Tondas[3], Muhammad Naufal Rachmatullah[1,2], Firdaus[1,2], Ade Iriani Sapitri[1,2], Anggun Islami[1,2], Sukemi[4], Muhammad Fachrurrozi[5], Siti Nurmaini[1,2], Rendy Isdwanta[1,2], Jordan Marcelino[1,2]
[1]Intelligent System Research Group, Faculty of Computer Science, Universitas Sriwijaya, Palembang, Indonesia
[2]Artificial Intelligence-Medical Center of Excellence, Universitas Sriwijaya, Palembang, Indonesia
[3]Department of Cardiology and Vascular Medicine, Dr. Mohammad Hoesin Hospital, Palembang, Indonesia
[4]Department of Computer System, Faculty of Computer Science, Universitas Sriwijaya, Palembang, Indonesia
[5]Department of Informatic Engineering, Faculty of Computer Science, Universitas Sriwijaya, Palembang, Indonesia

Article Info

Article history:

Received Apr 18, 2025
Revised Oct 21, 2025
Accepted Dec 6, 2025

Keywords:

Deep learning
Delineation
Electrocardiogram
Health
Myocardial infarction

ABSTRACT

ST-elevation or ST-depression are markers of an abnormal heart condition detected through an electrocardiogram (ECG) where the tracing in the ST-segment is unusually elevated above the TP-segment (baseline). Identifying the localization of the ST-segment on an ECG is difficult because even a minor change in the ST-segment can be obscured by filtering processes. The 12-lead ECG signal is a non-invasive tool in the early detection of ST-elevation based on ST- and TP-segment, with quick and accurate interpretation. This study proposes a standard 12-lead ECG delineation model using deep learning (DL). The ECG signal has been segmented to Pstart–Pend, Pend–QRSstart, QRSstart–Rpeak, Rpeak–QRSend, QRSend–Tstart, Tstart–Tend, and Tend–Pstart. The study interpreted ST-elevation or -depression using an ECG delineation approach guided by medical rules. The findings revealed that the DL model achieved an average accuracy of 99.18%, sensitivity of 92.55%, specificity of 99.55%, precision of 92.61%, and F1-score of 92.52% in limb leads. Similarly, in chest leads, the DL model attained an accuracy of 99.16%, sensitivity of 93.10%, specificity of 99.53%, precision of 93.32%, and F1-score of 93.11%. This study also validated the DL-predicted results by a cardiologist from Mohammad Hoesin Hospital, Indonesia.

This is an open access article under the CC BY-SA license.

Corresponding Author:

Annisa Darmawahyuni
Intelligent System Research Group, Faculty of Computer Science, Universitas Sriwijaya
Palembang, Indonesia
Email: riset.annisadarmawahyuni@gmail.com

1. INTRODUCTION

ST-elevation is a criterion for abnormal cardiac conditions, such as occlusion of coronary arteries in cases of acute myocardial infarction [1]. ST-elevation is not only associated with total thrombus blockage of the coronary vessels in myocardial infarction but is also associated with other conditions, such as ST-elevation in left bundle branch block (LBBB), pericarditis, and myocarditis [2], [3]. Consequently, its presence can lead to false-positive diagnoses in ST-elevation changes related to abnormal heart conditions [4].

Several deployed methods have been proposed for detecting ST-elevation, such as coronary angiography and echocardiography [4], [5]. However, the initial rule-out phase for ST-elevation is

inappropriate, as it can only be assessed for a brief period or requires invasive and/or resource-intensive methods [6], [7]. Twelve-lead electrocardiogram (ECG) signal is a non-invasive tool in the early detection of ST-elevation based on ST- and TP-segment, with quick and accurate interpretation [8], [9]. Different from arrhythmia detection, 12-lead or 15-lead ECG (standard 12-lead and three Frank leads ECG) observation is necessary for ST-elevation detection [10], [11]. Every lead of the ECG signal has information on three main waveforms, i.e., P, T-waves, and QRS-complexes. If the ST-segment is elevated, locating the J-point can be essential. The J-point is the junction of the QRS complex and the ST-segment. Therefore, the precise delineation of ECG is highly required to start, peak, and end of waveform localization for the ST-segment. ECG delineation plays a crucial role in determining the critical points that indicate the interval and amplitude locations in each wave morphology [12]. ECG delineation to ST-segment localization is challenging due to a slight alteration in the ST-segment that a filtering process could easily obliterate. In addition, the amplitude of ST-elevation may also be impacted by adjustments to the axis, QRS width, incorrect high-pass filter settings, and lead location [13].

However, prompt treatment depends on early detection and accurate diagnosis. Despite the established criteria for ST-elevation diagnosis, emergency clinicians still face a significant barrier to quickly identifying the condition. According to earlier studies, ranging from 2 to 30% of patients had an incorrect diagnosis of ST-elevation in myocardial infarction on the first medical contact [14]-[17]. Patients with ST-elevation who have high-risk ECG abnormalities not identified receive worse care and have more unfavorable outcomes. Misinterpreting a diagnostic test was found to be one of the main reasons for missed identification during the diagnostic procedure [14], [15]. Therefore, systematic methods to enhance ECG interpretation may significantly affect diagnosis. Since the 12-lead ECG is the primary diagnostic tool for ST elevation, a more thorough examination of the ECG could expedite the process considerably.

The current deep learning (DL) revolution has provided us with an opportunity to be effective in medical applications [4]-[6]. Many recent studies have explored ST-elevation with DL [8], [16]–[19]. However, the studies were only concerned with detecting or classifying the abnormalities, not observing the ST-segment changes to detect ST-elevation. For example, Choi *et al.* [8] proposed DL to train with ST-segment elevation myocardial infarction (STEMI) and normal sinus rhythm ECG for external validation. Tseng *et al.* [16] proposed DL to detect STEMI patients who underwent primary percutaneous coronary intervention (PCI). Wu *et al.* [17] detected the early diagnosis of acute STEMI with a convolutional neural network-long short-term memory. Gibson *et al.* [18] also proposed DL and compared DL-based 12-lead and one-lead ECGs to identify STEMI. Herman *et al.* [19] evaluated in an international cohort and compared with STEMI criteria and ECG experts in detecting occlusion myocardial infarction using the DL approach.

A signal delineation approach can be used to identify abnormalities in the ST-segment. In the previous study, a 12-lead ECG delineation model employing DL was proposed, which yielded exceptional performance outcomes [20]. To our knowledge, no studies have been conducted focusing on and addressing ST-segment changes for the assessment of ST-elevation or -depression condition through an ECG delineation approach. Therefore, in this study, the contributions and novelty are as follows:

- Generalizing the 12-lead ECG delineation approach using a DL model.
- Applying medical guidelines for accurate ST- and TP-segment localization and J-point determination to identify ST-elevation or -depression condition.
- Comparing DL-predicted ST-elevation, or -depression across the 12-lead with evaluations from two cardiologists at an Indonesian hospital.

2. MATERIAL AND METHODS

The research methodology of this study can be presented in Figure 1. The figure illustrates the overall workflow of an automated system for ECG abnormal interpretation and detection using DL methods. The process begins with the input of ECG 12-lead raw data, which captures the electrical activity of the heart over time. Since raw ECG signals often contain noise and variability, the data undergoes a pre-processing stage. After pre-processing, the signals proceed to the ECG waveform classification stage, which employs a ConvBiLSTM architecture. This architecture integrates convolutional neural network (CNN) with bidirectional long short-term memory (BiLSTM) networks to capture both spatial and temporal features of the ECG signals.

2.1. Data preparation

Twelve-lead ECG signals with annotations for P, T, and QRS-complexes are included in the Lobachevsky University Electrocardiography Database (LUDB) [21]. Total of 500 samples per second are used to digitize the 200 10-second records. 19,666 T-waves, 21,966 QRS-complexes, and 16,797 P-waves are annotated. This study has generated the 12-lead ECG delineation model with 200 records and a complete P-QRS-T waveform. Figure 2 presents a sample of ST-elevation conditions in ECG records.

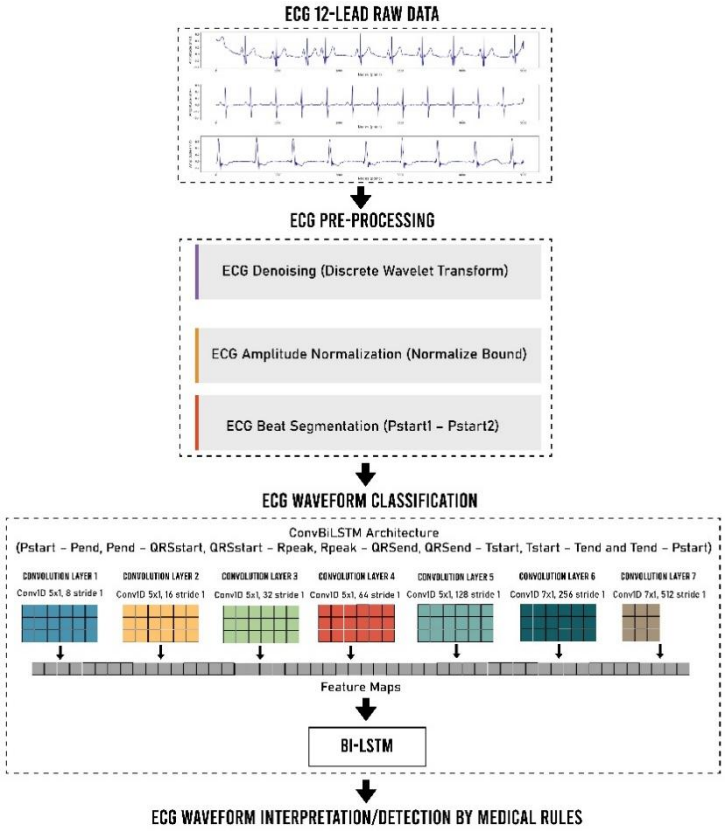

Figure 1. The research method

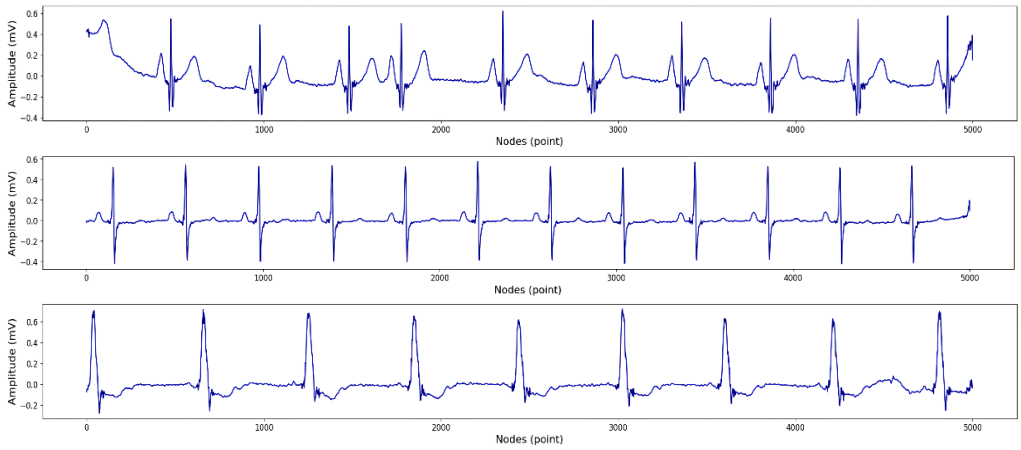

Figure 2. The sample of the ST-elevation [21]

2.2. Electrocardiogram signal processing

There are steps to process the ECG signal so that its information is well-represented. The processing of ECG signals is described below:

– ECG denoising: ECG is susceptible to noises due to it representing varying morphological waves. It leads to a false diagnosis and improper patient treatment. Discrete wavelet transforms (DWT) have been proposed in previous literature to handle ECG denoising problems [20], [22], [23]. This study has explored several mother functions to obtain the highest signal-to-noise ratio (SNR) value, i.e., *haar*, *bior5.5*, *bior3.3*, *bior6.8*, *coif2*, *coif4*, *coif5*, *sym4*, *sym5*, *sym6*, *sym7*, *db8*, *db9*, *coif3*, *db7*, and *db6*. Among explored mother functions, the highest SNR value achieves 34.71 decibels (dB), with *bior6.8* mother function, soft thresholding, and seven levels of decomposition. The sample of ECG denoising can be presented in Figure 3.

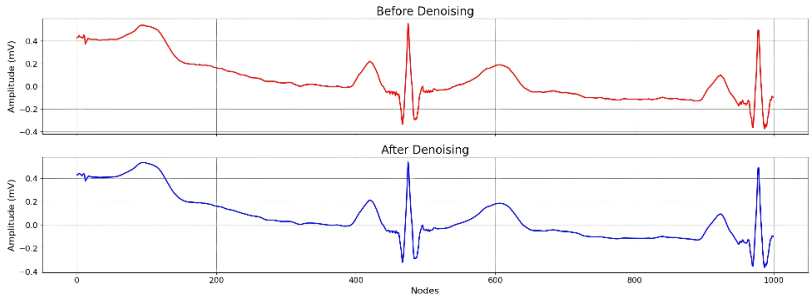

Figure 3. The sample of ECG denoising

– ECG segmentation: this study has segmented the ECG signal in 12-lead by beat-to-beat, with the maximum nodes in all ECG leads being 816, as the minimum beat among all records. This study has only segmented the complete P-QRS-T waveforms (normal beat). If the beat segment is less than 816 nodes, we used the zero-padding technique. This study has added zeros to the end of the input sequence so that the beat segmentation has a fixed length.

2.3. The modified ConvBiLSTM model

Our previous study introduced a 12-lead ECG delineation model using DL, which demonstrated outstanding performance [20], [23], [24]. However, the study focused solely on delineating the P-QRS-T waves with four classes (i.e., P-wave, QRS-complex, T-wave, and isoelectric line), without addressing ST-elevation or -depression. This omission is significant, as these conditions are critical indicators of various heart diseases like STEMI. Building upon this foundation [20], this study has refined the previous methodology CNN-BiLSTM in terms of ST- and TP-segments localization for detecting both ST-elevation and -depression. The generalization of the previous model was called modified ConvBiLSTM. To carry out this process, the classification is changed into eight classes (i.e., P_{start}–P_{end}, P_{end}–QRS_{start}, QRS_{start}–R_{peak}, R_{peak}–QRS_{end}, QRS_{end}–T_{start}, T_{start}–T_{end}, T_{end}–P_{start}, and isoelectric line) to determine the J-point as seen from the ST-segment and TP-segment. A total of 816 nodes, which was the beat-to-beat segmentation in a 12-lead ECG signal was used for input. One-dimensional CNNs have seven convolutional layers, with a kernel size of five with stride one. The rectified linear unit (ReLU) function was adopted with 8, 16, 32, 64, 128, 256, and 512 filters. The other hyperparameters tuning are RMSprop optimizer, batch size of 32, 300 epochs, and 10^{-3} learning rate. Table 1 lists the details of the modified model.

Table 1. The description of the modified ConvBiLSTM model

Layer	Input nodes	Number of filters	Kernel size/dropout rate	Output nodes	Kernel regularizer
Input	816×1	-	-	-	-
Convolution 1	816×1	8	5×1, stride 1	816×8	-
Normalization 1	816×8	-	-	816×8	-
ReLU 1	816×8	-	-	816×8	-
Convolution 2	816×8	16	5×1, stride 1	816×16	-
Normalization 2	816×16	-	-	816×16	-
ReLU 2	816×16	-	-	816×16	-
Convolution 3	816×16	32	5×1, stride 1	816×32	-
Normalization 3	816×32	-	-	816×32	-
ReLU 3	816×32	-	-	816×32	-
Convolution 4	816×32	64	5×1, stride 1	816×64	-
Normalization 4	816×64	-	-	816×64	-
ReLU 4	816×64	-	-	816×64	-
Convolution 5	816×64	128	5×1, stride 1	816×128	-
Normalization 5	816×128	-	-	816×128	-
ReLU 5	816×128	-	-	816×128	-
Convolution 6	816×128	256	7×1, stride 1	816×256	L2(α=0.0001)
Normalization 6	816×256	-	-	816×256	-
ReLU 6	816×256	-	-	816×256	-
Convolution 7	816×256	512	7×1, stride 1	816×512	L2(α=0.0001)
Normalization 7	816×512	-	-	816×512	-
ReLU 7	816×512	-	-	816×512	-
Dropout 1	816×512	-	0.3	816×512	-
BiLSTM	816×512	-	-	816×1556	L2(α=0.0001)
Fully connected	816×1556	-	-	816×512	L2(α=0.0001)
Dropout 2	816×512	-	0.3	816×512	-
Output	816×512	-	-	816×8	-

2.4. ST-elevation or ST-depression decision

The medical rules of ST-elevation or ST-depression [25], [26], this study has summarized as below:

- ST-elevation is measured at the J-point (QRS_{off} and the beginning of ST-segment) compared to the baseline which is TP-segment (T_{off}–P_{on}). TP segment is between the end of the T wave and the next P wave. TP segment is truly isoelectric and hence the true baseline for all ECG measurements, while the other two segments may have deviations from the baseline. In conclusion, if J-point is higher than the baseline by 0.1 mV, it is called ST-elevation.
- ST-depression is measured by the J-point is below the baseline.

To adjust those rules, this study has followed a basic principle of ECG analysis, in which each 1 millimeter (mm) in an ECG small square corresponds to 0.04 seconds (40 milliseconds) [25]. The amplitude of waveforms will be expressed as: 0.1 mV=1 mm=1 small square [26].

2.5. Platform

Two NVIDIA GeForce RTX 2070 SUPER 24GB GPUs (8 GB Dedicated and 16 GB Shared) and an Intel(R) Core (TM) I7-10700K CPU operating at 3.80 GHz (16 CPUs) ~3.8 GHz are used in the experiments to create the 12-lead ECG delineation model. Python programming with Visual Studio Code version 1.86.1 on Windows 10 Pro 64 Bit was used in this study. Numpy, pandas, matplotlib, seaborn, wfdb, pywavelets, SciPy, and TensorFlow are among the libraries.

3. RESULTS AND DISCUSSION

Total of 200 records in all have been divided into beat-to-beat categories. There are 14,615 normal beats in total, divided into 1,470 beats for the validation set, 1,468 beats for the testing set (unseen), and 11,677 beats for the training set (see Table 2). Table 2 presents the total number of segmented ECG beats across 12 standard leads (I, II, III, aVR, aVL, aVF, and V1–V6), categorized into training, validation, and testing datasets. The dataset shows a well-structured segmentation of ECG beats, with a dominant portion allocated for training and equal-sized portions for validation and testing. The beat distribution is fairly uniform across all leads, supporting robust and unbiased model training and evaluation. To analyze the performance results of the modified ConvBiLSTM model, this study has discussed two approaches: i) 12-lead ECG delineation and ii) ST-elevation detection.

Table 2. The total number of beat-to-beat segmentation

Data	Total number of beats segmentation											
	I	II	III	aVR	aVL	aVF	V1	V2	V3	V4	V5	V6
Training set	977	975	979	975	977	975	967	967	971	967	975	972
Validation set	123	123	123	123	123	123	122	122	122	122	122	122
Testing set	123	122	123	123	123	123	122	121	122	122	122	122
Total beats	1,223	1,220	1,225	1,221	1,223	1,221	1,211	1,210	1,215	1,211	1,219	1,216

3.1. Delineation result

The myocardial mass may have an impact on the waveform's amplitude in any lead. Six limb leads (I, II, III, aVR, aVL, and aVF) plus six chest leads (VI–V6) make up a typical 12-lead ECG. The vertical heart view is produced by six limb leads, whereas the horizontal heart image is presented by six chest leads [27]. In this study, we have analyzed the performance results of limb and chest leads, respectively (refer to Tables 3 and 4). On average, the performance results of the chest lead outperformed the limb leads in sensitivity, precision, and F1-score with 93.10%, 93.32%, and 93.11%, respectively. However, in accuracy and specificity, the limb leads outperformed. In limb leads, leads I-III show better performance than lead aVR, aVL, and aVF with above 92.53% accuracy, sensitivity, specificity, precision, and F1-score. Lead aVR shows poor performance, with only 88.87% F1-score. In chest leads, lead V1 only obtains 91.19% sensitivity, while in lead V2–V3 is well-performed. As anatomical relations of lead in 12-lead ECG, leads aVR and V1 have the same anatomy which presents the right atrium and cavity of the left ventricle. In some cases, lead aVR is ignored, due to its locations displaying reciprocal information covered by leads aVL, II, V5, and V6.

In all 12-ECG leads, T_{on}–T_{off} and T_{off}–P_{on} had the highest misclassification rates, as seen in the confusion matrix (CM) in Figures 4(a) to (l) (see Appendix). From both the mathematical and the cardiological points of view, the maximal error is noted for the T_{off}, whose delineation is a well-known hard problem. A normal T-wave to overlap with other T-wave classes: inverted, only upwards, only downwards, biphasic negative-positive, or biphasic positive-negative. The T-wave on an ECG is significant because it shows cardiac repolarization. The correct interpretation of T-waves can aid in the prediction of cardiac events

in patients. Though the misclassification mostly occurs in T_{on}–T_{off} and T_{off}–P_{on}, this study has minimized the error classification in ST-segment (QRS_{off}–T_{on}) and PR-segment (P_{off}–QRS_{on}). Both segments are significant features for ST-elevation detection.

Table 3. The performance results of limb lead delineation

Metrics	Performance results (%)						Average
	I	II	III	aVR	aVL	aVF	
Accuracy	99.36	99.3	99.11	99.05	99.11	99.12	99.18
Sensitivity	94.43	94.33	93.31	88.91	91.26	93.05	92.55
Specificity	99.65	99.62	99.51	99.49	99.5	99.51	99.55
Precision	94.28	93.91	92.53	89.02	92.46	93.48	92.61
F1-score	94.34	94.08	92.81	88.87	91.79	93.24	92.52

Table 4. The performance results of chest lead delineation

Metrics	Performance results (%)						Average
	V1	V2	V3	V4	V5	V6	
Accuracy	98.95	99.08	99.28	99.02	99.3	99.34	99.16
Sensitivity	91.52	91.64	94.01	93.01	94.01	94.38	93.10
Specificity	99.43	99.5	99.6	99.44	99.6	99.63	99.53
Precision	91.19	91.7	93.7	93.32	95.2	94.79	93.32
F1-score	91.24	91.59	93.77	93.01	94.47	94.55	93.11

Figure 5 shows the ECG delineation results of P_{start}–P_{end}, P_{end}–QRS_{start}, QRS_{start}–R_{peak}, R_{peak}–QRS_{end}, QRS_{end}–T_{start}, T_{start}–T_{end}, and T_{end}–P_{start} in limb and chest leads, respectively. All lead's physical characteristics affect how well delineation works. The degree of morphological alterations depends on the shift's magnitude, displacement's direction, and the ECG segment chosen for analysis. Each lead represents the difference in electrical potentials between two places in space.

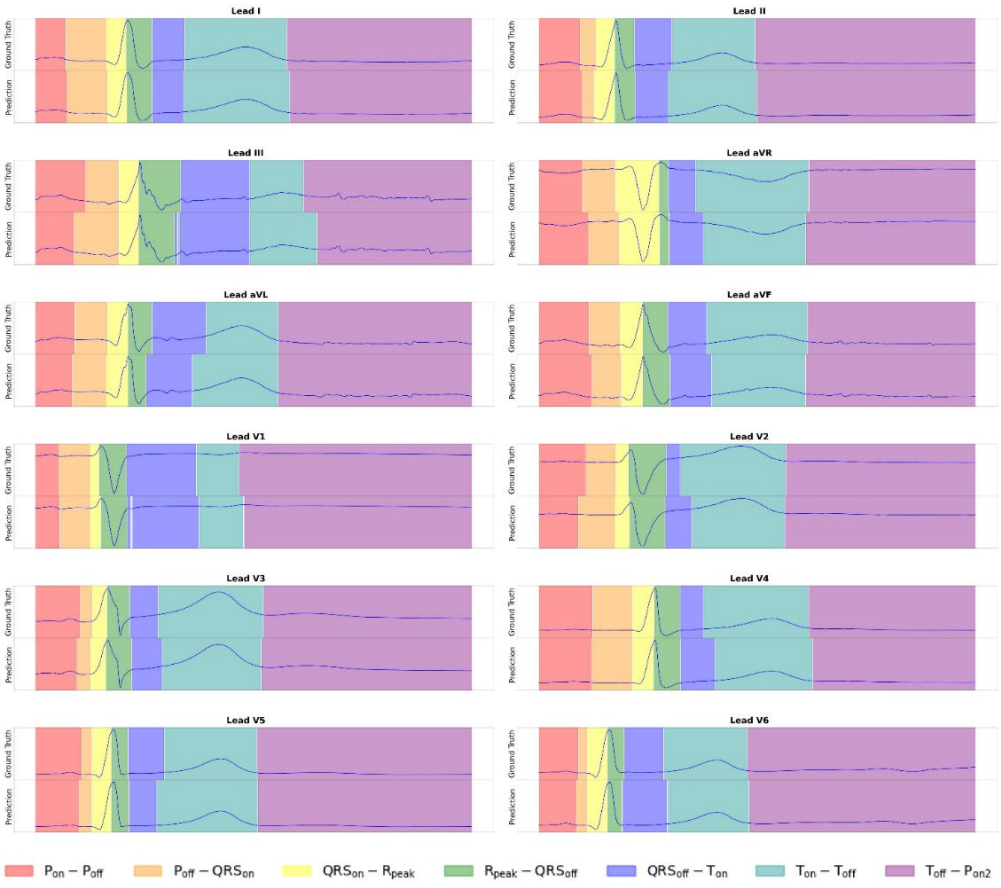

Figure 5. The comparison of ECG signal classification between ground truth (annotation) and predicted ConvBiLSTM results in limb leads

3.2. ST-elevation or ST-depression condition

We have implemented the medical rules for ST-elevation or ST-depression in ECG signals. We have only used the medical rules for several annotated records of LUDB. For ST-elevation or ST-depression detection, we used the eight LUDB records, i.e., records 7, 21, 24, 33, 55, 64, 69, and 86. The records have patient information, including demography and medical data, with the ST-elevation myocardial infarction condition. A detailed description of the used records for ST-elevation or -depression detection is listed in Table 5. The sample results of ST-elevation (red color) as E, ST-depression (green color) as D, and neither (blue color) as N in records 7, 24, and 33 of the 12-lead ECG signals (only sample visualized). For ST-elevation, the J-point is higher than the baseline by 0.1 mV, and for ST-depression, the J-point is below the baseline. ST-elevation is measured at the J-point (QRS_{off} and the beginning of the ST-segment) compared to the baseline, which is the TP-segment (T_{off}–P_{on}).

Table 5. The sample of ST-elevation or -depression decision by medical rules with DL localization

Records	Sex	Age	Results
7	Male	50	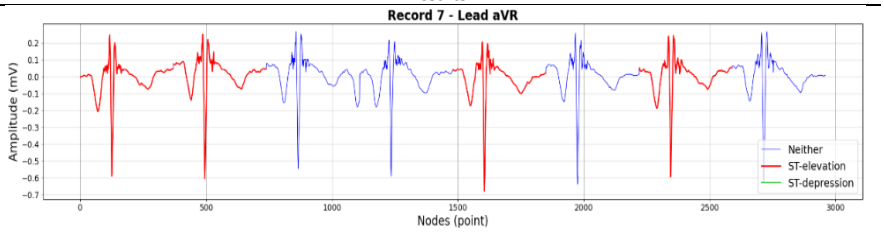 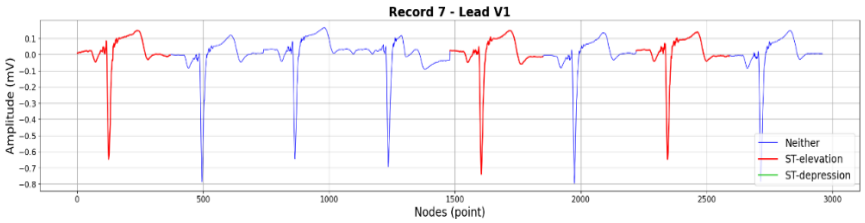
24	Male	64	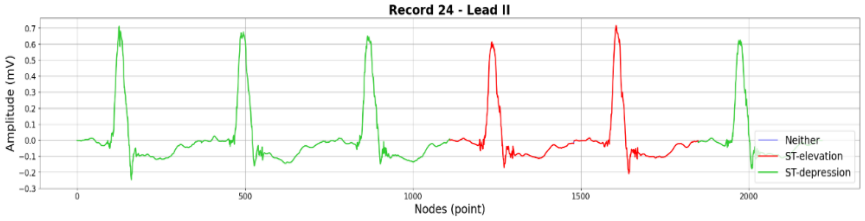 
33	Male	53	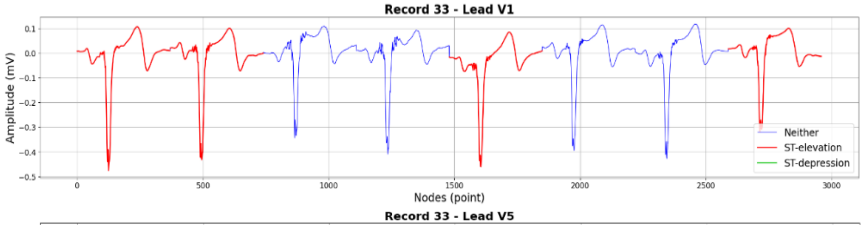 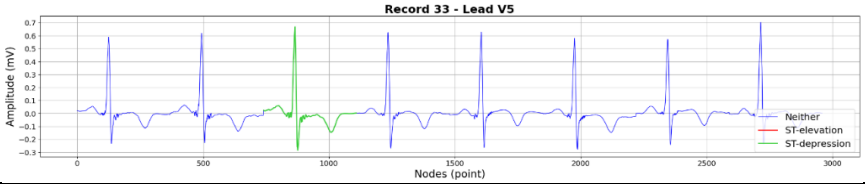

The study has validated the DL-predicted results against those of a cardiologist from Mohammad Hoesin Hospital, Indonesia. As a result, we have taken four records as samples, among the 48 ECG signals from eight records (records 7, 21, 24, and 33) in 12-lead ECG signals, 35 records showed interpretation results that

matched those of the cardiologist. The validation results are listed in Table 6. There were six false interpretations, specifically, in record 7, at leads aVR and V2, in record 24, at leads V4 and V5, and in record 33, at leads II and V2. In the automatic delineation process, for the QRS complex, a relatively simple task, the performance of all methods is next to perfect. However, the most significant error occurs in delineating the T-wave start and end, a widely recognized challenging task from both mathematical and cardiological standpoints [21]. The presence of T-wave inversion can be the main challenge for ST-segment localization in this study.

Table 6. The validation results by an Indonesian cardiologist of 12-lead ECG signal decision

Records	Lead	Indonesian cardiologist	DL-predicted	Results
7	aVF	N	N	True
	aVL	D	D	True
	aVR	N	E	False
	I	D	D	True
	II	N	N	True
	III	N	N	True
	V1	E	E	True
	V2	E	N	False
	V3	E	E	True
	V4	E	E	True
	V5	N	N	True
	V6	D	D	True
21	aVF	N	D	False
	aVL	N	D	False
	aVR	N	N	True
	I	N	D	False
	II	N	N	True
	III	N	D	False
	V1	E	N	False
	V2	E	N	False
	V3	E	E	True
	V4	E	N	False
	V5	E	E	True
	V6	N	N	True
24	aVF	N	N	True
	aVL	D	D	True
	aVR	E	E	True
	I	D	D	True
	II	D	D	True
	III	N	N	True
	V1	E	E	True
	V2	E	E	True
	V3	E	E	True
	V4	D	E	False
	V5	D	N	False
	V6	D	D	True
33	aVF	N	N	True
	aVL	D	D	True
	aVR	N	N	True
	I	D	D	True
	II	N	D	False
	III	N	N	True
	V1	E	E	True
	V2	E	N	False
	V3	N	N	True
	V4	N	N	True
	V5	N	N	True
	V6	N	N	True

The 12-lead ECG delineation in Table 7 has been the subject of prior research [9], [20], [28]. CNN-BiLSTM was initially proposed by S. and B. [20] for 12-lead ECG delineation. They outperformed 95% for beat-based segmentation and 93% for patient-based segmentation in terms of accuracy, sensitivity, specificity, precision, and F1-score, based on a total of 14,588 beats. The W-Net architecture, which applies a second U-Net with the input being the first U-Net's output, was examined by Jimenez-Perez *et al.* [9]. They used the efficient channel attention (ECA) method to address the trade-off between complexity and performance. They experimented with both single-lead and multi-lead methods for ECG delineation. The precision for P, QRS, and T waves in the single-lead configuration was 99.27%, 99.31%, and 98.73%, respectively. The precision decreased to 98.90%, 99.24%, and 98.24% for P, QRS, and T waves,

respectively, when the model was used with the multi-lead technique. Chen *et al*. [28] used a one-dimensional UNet architecture (1D-UNet) to define three primary ECG waveforms. They achieved a 98.86% sensitivity.

Table 7. The comparison results of multi-lead or 12-lead ECG delineation based on DL architectures

Authors	Dataset	Lead	Method	Performance results (%)				
				ACC	SEN	SPE	PRE	F1
[9]	LUDB	Multi-lead	W-Net	-	99.93	-	99.87	-
[20]	LUDB	12	CNN-BiLSTM	98.82	95.93	99.21	95.94	95.93
[28]	LUDB	12	1D-UNet	-	98.86	-	-	-
This study	LUDB	Limb lead	A modified ConvBiLSTM	99.18	92.55	99.55	92.61	92.52
		Chest lead		99.16	93.10	99.53	93.32	93.11

Prior studies demonstrated excellent performance in ECG wave delineation but were limited to P-QRS-T wave analysis. They did not focus on segments crucial for detecting abnormalities, such as ST-elevation and ST-depression, which are essential indicators of conditions like myocardial infarction. The study extends ECG segmentation beyond just P-QRS-T waves by defining finer wave intervals and segments; P_{start}–P_{end}, P_{end}–QRS_{start}, QRS_{start}–R_{peak}, R_{peak}–QRS_{end}, QRS_{end}–T_{start}, T_{start}–T_{end}, and T_{end}–P_{start}. The findings revealed that the DL model achieved an average accuracy of 99.18%, sensitivity of 92.55%, specificity of 99.55%, precision of 92.61%, and F1-score of 92.52% in limb leads. Similarly, in chest leads, the DL model attained an accuracy of 99.16%, sensitivity of 93.10%, specificity of 99.53%, precision of 93.32%, and F1-score of 93.11%. These refined segments allow for a more detailed understanding of ECG morphology, improving abnormality detection. Interpretation of ST-elevation or -depression is guided by medical rules, ensuring that the model aligns with clinical practices. This study enhances ECG segmentation by incorporating additional clinically relevant segments for abnormality detection. The DL model exhibits strong accuracy and reliability, with high specificity, indicating a low false-positive rate.

4. CONCLUSION

ST-elevation or ST-depression are conditions of ST-segment of the lead with the injured area as a positive and negative electrode, respectively. With the 12-lead ECG delineation approach, this study is concerned with detecting the ST-elevation or -depression based on ST- and TP-segment localization. Both ECG segments have been compared to J-point localization, with a standard amplitude of 0.1 mV. To reach the aim of this study, we modified the ECG processing to ST-segment localization for ST-elevation or -depression detection in 12-lead ECG (limb and chest leads). For ST-elevation, the J-point is higher than the baseline by 0.1 mV, and for ST-depression, the J-point is below the baseline. We segment the ECG signal to P_{start}–P_{end}, P_{end}–QRS_{start}, QRS_{start}–R_{peak}, R_{peak}–QRS_{end}, QRS_{end}–T_{start}, T_{start}–T_{end}, and T_{end}–P_{start}. As a results, on average, the performance results of ECG delineation in the chest lead outperformed the limb leads in sensitivity, precision, and F1-score with 93.10%, 93.32%, and 93.11%, respectively. Future work may involve integrating the proposed ST-segment delineation method with automated diagnostic systems to assist clinicians in real-time detection of myocardial infarction or ischemia.

ACKNOWLEDGMENTS

We thank the Intelligent System Research Group (ISysRG), Faculty of Computer Science and Artificial Intelligence-Medical Center of Excellence, Universitas Sriwijaya, 30139, Palembang, Indonesia, for the DL infrastructure.

FUNDING INFORMATION

This study is funded by Universitas Sriwijaya, Indonesia under a Professional Grant 2024 Number 0125.035/UN9/SB3.LP2M.PT/2024. This study is also funded by the Indonesian Endowment Fund for Education (LPDP) on behalf of the Indonesian Ministry of Higher Education, Science and Technology and managed under the EQUITY Program (Contract Numbers 4316/B3/DT.03.08/2025 and 66/UN9/PKS/2025 which made this research process possible.

AUTHOR CONTRIBUTIONS STATEMENT

This journal uses the Contributor Roles Taxonomy (CRediT) to recognize individual author contributions, reduce authorship disputes, and facilitate collaboration.

Name of Author	C	M	So	Va	Fo	I	R	D	O	E	Vi	Su	P	Fu
Bambang Tutuko	✓								✓					
Annisa Darmawahyuni		✓							✓					
Alexander Edo Tondas						✓				✓				
Muhammad Naufal Rachmatullah			✓		✓					✓				
Firdaus						✓	✓			✓				
Ade Iriani Sapitri						✓	✓			✓				
Anggun Islami					✓		✓			✓				
Sukemi					✓		✓			✓				
Muhammad Fachrurrozi					✓		✓			✓				
Siti Nurmaini					✓					✓		✓		✓
Rendy Isdwanta		✓	✓				✓			✓				
Jordan Marcelino		✓	✓							✓				

C : **C**onceptualization
M : **M**ethodology
So : **So**ftware
Va : **Va**lidation
Fo : **Fo**rmal analysis
I : **I**nvestigation
R : **R**esources
D : **D**ata Curation
O : Writing - **O**riginal Draft
E : Writing - Review & **E**diting
Vi : **Vi**sualization
Su : **Su**pervision
P : **P**roject administration
Fu : **Fu**nding acquisition

CONFLICT OF INTEREST STATEMENT

The authors have no conflicts of interest.

DATA AVAILABILITY

The datasets generated and/or analysed during the current study are available in the PhysioNet:Lobachevsky University Electrocardiography Database repository (https://physionet.org/content/ludb/1.0.1/).

REFERENCES

[1] M. G. Del Buono *et al.*, "Heart Failure After ST-Elevation Myocardial Infarction: Beyond Left Ventricular Adverse Remodeling," *Current Problems in Cardiology*, vol. 48, no. 8, p. 101215, Aug. 2023, doi: 10.1016/j.cpcardiol.2022.101215.

[2] K. Nikus, Y. Birnbaum, M. Fiol-Sala, J. Rankinen, and A. B. de Luna, "Conduction Disorders in the Setting of Acute STEMI," *Current Cardiology Reviews*, vol. 17, no. 1, pp. 41–49, Jan. 2021, doi: 10.2174/1573403x16666200702121937.

[3] L. H. Mughal and S. Sastry, "Advances in the treatment of ST Elevation Myocardial Infarction in the UK," *JRSM Cardiovascular Disease*, vol. 11, Jan. 2022, doi: 10.1177/20480040221075519.

[4] E. Radwa, H. Ridha, and B. Faycal, "Deep learning-based approaches for myocardial infarction detection: A comprehensive review recent advances and emerging challenges," *Medicine in Novel Technology and Devices*, vol. 23, 2024, doi: 10.1016/j.medntd.2024.100322.

[5] N. Iwahashi *et al.*, "Global Strain Measured by Three-Dimensional Speckle Tracking Echocardiography Is a Useful Predictor for 10-Year Prognosis after a First ST-Elevation Acute Myocardial Infarction," *Circulation Journal*, vol. 85, no. 10, pp. 1735–1743, Sep. 2021, doi: 10.1253/circj.CJ-21-0183.

[6] R. Xiao, Y. Xu, M. M. Pelter, D. W. Mortara, and X. Hu, "A Deep Learning Approach to Examine Ischemic ST Changes in Ambulatory ECG Recordings," in *AMIA Joint Summits on Translational Science Proceedings*, 2018, vol. 2017, pp. 256–262.

[7] J. O. Emakhu, "Acute Coronary Syndrome Prediction: A Data-Driven Machine Learning Modeling Approach in Emergency Care," M.S. thesis, Wayne State University, Detroit, MI, USA, 2022.

[8] H. Y. Choi *et al.*, "Diagnostic Accuracy of the Deep Learning Model for the Detection of ST Elevation Myocardial Infarction on Electrocardiogram," *Journal of Personalized Medicine*, vol. 12, no. 3, p. 336, Feb. 2022, doi: 10.3390/jpm12030336.

[9] G. Jimenez-Perez, J. Acosta, A. Alcaine, and O. Camara, "Generalising electrocardiogram detection and delineation: training convolutional neural networks with synthetic data augmentation," *Frontiers in Cardiovascular Medicine*, vol. 11, Jul. 2024, doi: 10.3389/fcvm.2024.1341786.

[10] Y. Zhao *et al.*, "Early detection of ST-segment elevated myocardial infarction by artificial intelligence with 12-lead electrocardiogram," *International Journal of Cardiology*, vol. 317, pp. 223–230, Oct. 2020, doi: 10.1016/j.ijcard.2020.04.089.

[11] A. Darmawahyuni *et al.*, "Deep learning with a recurrent network structure in the sequence modeling of imbalanced data for ECG-rhythm classifier," *Algorithms*, vol. 12, no. 6, p. 118, Jun. 2019, doi: 10.3390/a12060118.

[12] S. Varaganti, R. L. Manisha, and S. Muvvala, "From Waves to Diagnoses: Decoding Electrocardiogram for Improved Cardiac Care," *Archives of Medicine and Health Sciences*, vol. 12, no. 1, pp. 88–96, Jan. 2024, doi: 10.4103/amhs.amhs_169_23.

[13] S. J. Perkins *et al.*, "Vectorcardiography Predicts Heart Failure in Patients Following ST Elevation Myocardial Infarction," *Annals of Noninvasive Electrocardiology*, vol. 29, no. 5, Sep. 2024, doi: 10.1111/anec.70013.

[14] J. McLaren, J. N. de Alencar, E. K. Aslanger, H. P. Meyers, and S. W. Smith, "From ST-Segment Elevation MI to Occlusion MI: The New Paradigm Shift in Acute Myocardial Infarction," *JACC: Advances*, vol. 3, no. 11, 2024, doi: 10.1016/j.jacadv.2024.101314.

[15] M. Ayyad *et al.*, "Reevaluating STEMI: The Utility of the Occlusive Myocardial Infarction Classification to Enhance Management of

Acute Coronary Syndromes," *Current Cardiology Reports*, vol. 27, no. 1, p. 75, 2025, doi: 10.1007/s11886-025-02217-8.
[16] L. M. Tseng, C. Y. Chuang, S. K. Chua, and V. S. Tseng, "Identification of Coronary Culprit Lesion in ST Elevation Myocardial Infarction by Using Deep Learning," *IEEE Journal of Translational Engineering in Health and Medicine*, vol. 11, pp. 70–79, 2023, doi: 10.1109/JTEHM.2022.3227204.
[17] L. Wu *et al.*, "Deep Learning Networks Accurately Detect ST-Segment Elevation Myocardial Infarction and Culprit Vessel," *Frontiers in Cardiovascular Medicine*, vol. 9, Mar. 2022, doi: 10.3389/fcvm.2022.797207.
[18] C. M. Gibson *et al.*, "Evolution of single-lead ECG for STEMI detection using a deep learning approach," *International Journal of Cardiology*, vol. 346, pp. 47–52, Jan. 2022, doi: 10.1016/j.ijcard.2021.11.039.
[19] R. Herman *et al.*, "International evaluation of an artificial intelligence-powered electrocardiogram model detecting acute coronary occlusion myocardial infarction," *European Heart Journal - Digital Health*, vol. 5, no. 2, pp. 123–133, 2024, doi: 10.1093/ehjdh/ztad074.
[20] S. V. S. and M.-P. T.B., "Meta-Heuristic Enhanced Deep Learning Model for Mango Blossom and Stem Disease Classification," *Journal of Artificial Intelligence and Capsule Networks*, vol. 7, no. 2, pp. 94–106, Jun. 2025, doi: 10.36548/jaicn.2025.2.001.
[21] A. Darmawahyuni *et al.*, "Improved delineation model of a standard 12-lead electrocardiogram based on a deep learning algorithm," *BMC Medical Informatics and Decision Making*, vol. 23, no. 1, p. 139, Jul. 2023, doi: 10.1186/s12911-023-02233-0.]
[22] A. I. Kalyakulina *et al.*, "LUDB: A new open-access validation tool for electrocardiogram delineation algorithms," *IEEE Access*, vol. 8, pp. 186181–186190, 2020, doi: 10.1109/ACCESS.2020.3029211.
[23] S. Nurmaini *et al.*, "Beat-to-Beat Electrocardiogram Waveform Classification Based on a Stacked Convolutional and Bidirectional Long Short-Term Memory," *IEEE Access*, vol. 9, pp. 92600–92613, 2021, doi: 10.1109/ACCESS.2021.3092631.
[24] S. Nurmaini *et al.*, "Robust electrocardiogram delineation model for automatic morphological abnormality interpretation," *Scientific Reports*, vol. 13, no. 1, p. 13736, Aug. 2023, doi: 10.1038/s41598-023-40965-1.
[25] A. H. Kashou *et al.*, "ECG Interpretation Proficiency of Healthcare Professionals," *Current Problems in Cardiology*, vol. 48, no. 10, p. 101924, Oct. 2023, doi: 10.1016/j.cpcardiol.2023.101924.
[26] C. J. Breen, G. P. Kelly, and W. G. Kernohan, "ECG interpretation skill acquisition: A review of learning, teaching and assessment," *Journal of Electrocardiology*, vol. 73, pp. 125–128, Jul. 2022, doi: 10.1016/j.jelectrocard.2019.03.010.
[27] A. L. Goldberger, Z. D. Goldberger, and A. Shvilkin, *Goldberger's Clinical Electrocardiography: A Simplified Approach*, 9th ed. 2017.
[28] Z. Chen, M. Wang, M. Zhang, W. Huang, H. Gu, and J. Xu, "Post-processing refined ECG delineation based on 1D-UNet," *Biomedical Signal Processing and Control*, vol. 79, p. 104106, Jan. 2023, doi: 10.1016/j.bspc.2022.104106.

APPENDIX

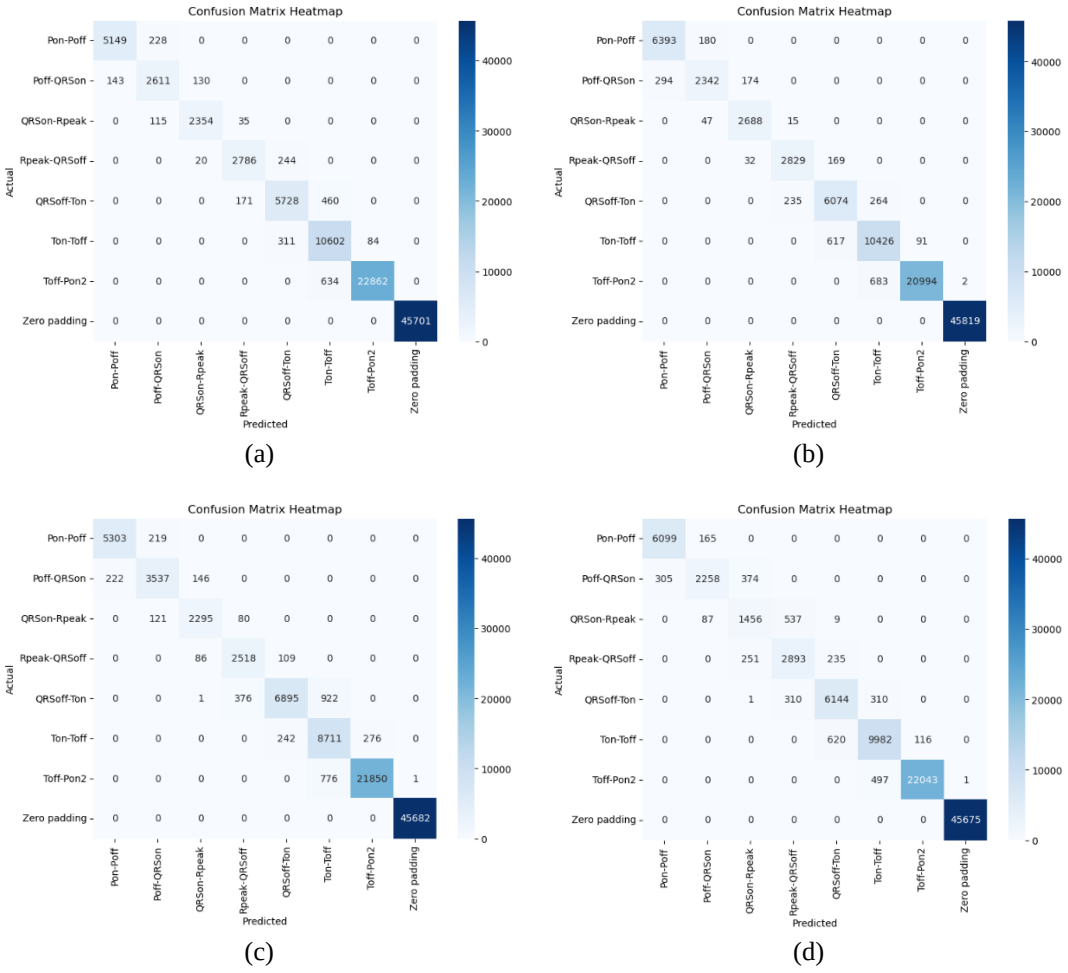

Figure 4. Confusion matrix of validation set in 12-lead ECG; (a) Lead I, (b) Lead II, (c) Lead III, and (d) Lead aVR

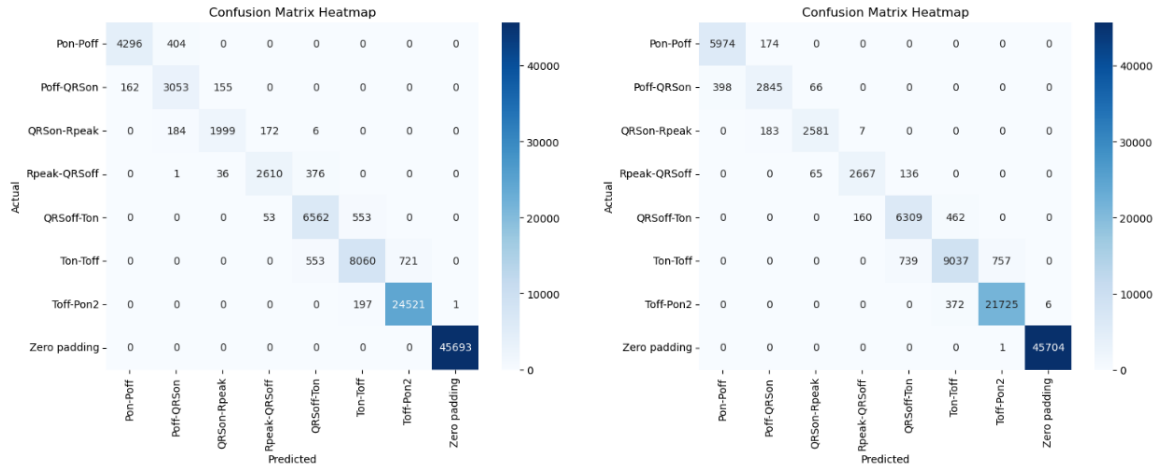

(e) (f)

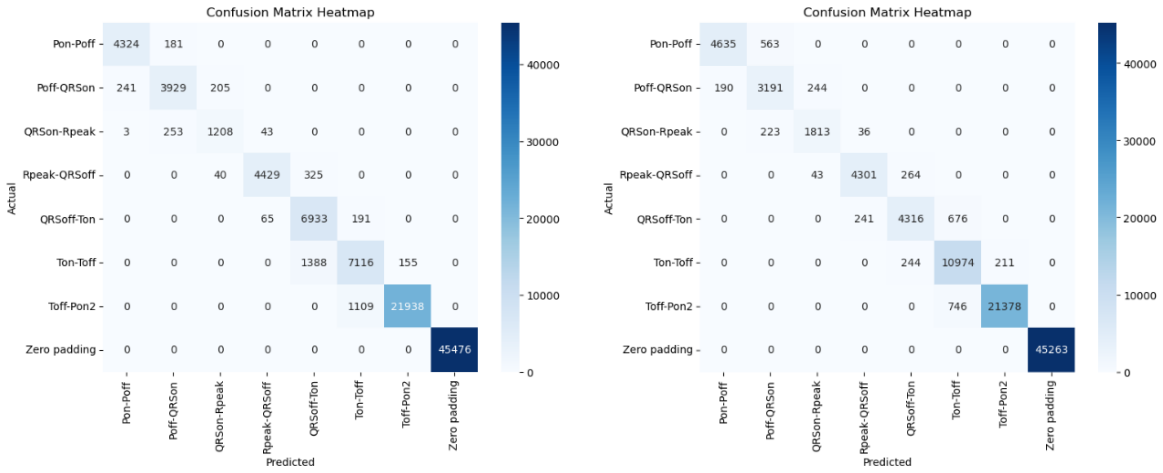

(g) (h)

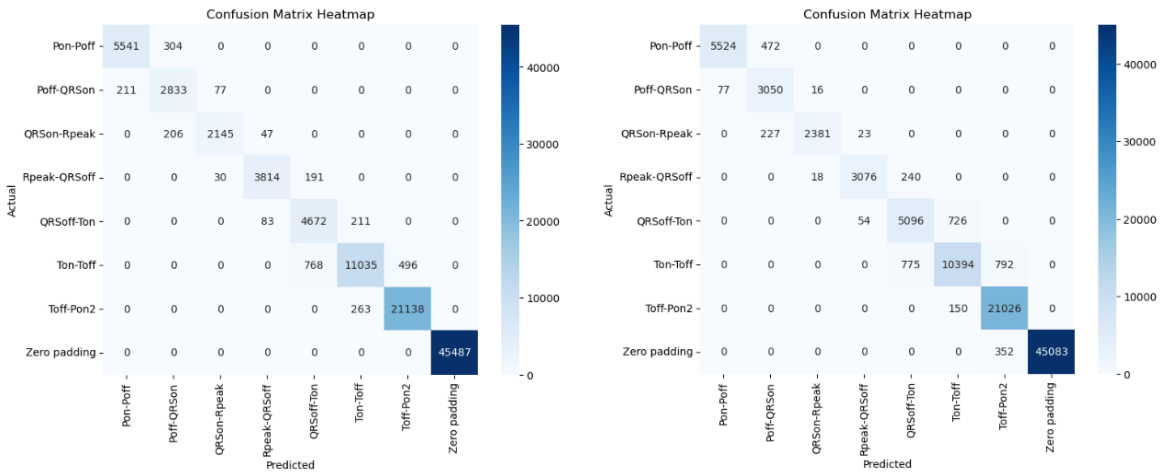

(i) (j)

Figure 4. Confusion matrix of validation set in 12-lead ECG; (e) Lead aVL, (f) Lead aVF, (g) Lead V1, (h) Lead V2, (i) Lead V3, and (j) Lead V4 (*continued*)

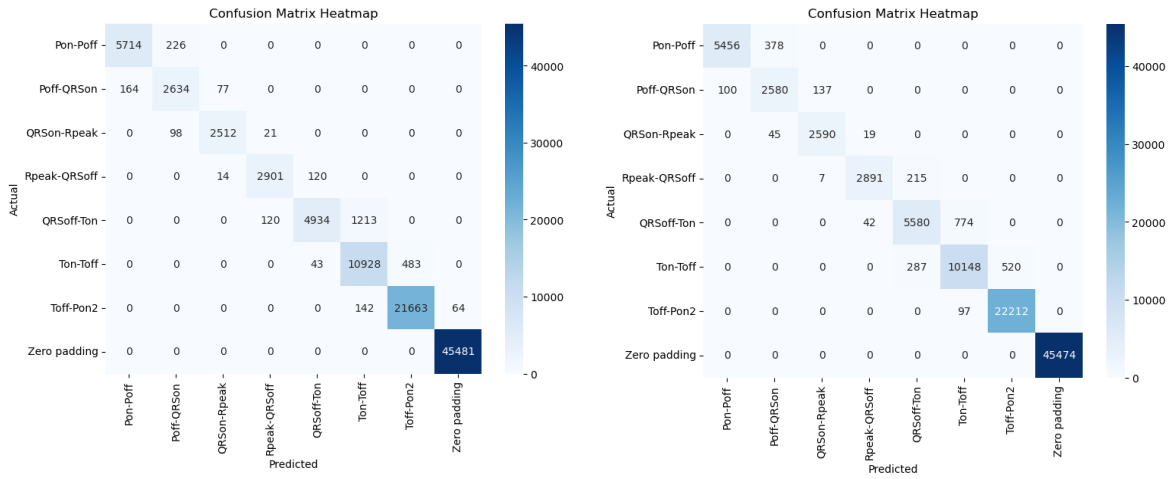

(k) (l)

Figure 4. Confusion matrix of validation set in 12-lead ECG; (k) Lead V5 and (l) Lead V6 (*continued*)

BIOGRAPHIES OF AUTHORS

Bambang Tutuko is currently a professor and researcher in the artificial intelligence-medical center of excellence, Universitas Sriwijaya, Palembang, Indonesia. His research interests include robotics, deep learning, and machine learning. He can be contacted at email: bambangtutuko60@gmail.com.

Annisa Darmawahyuni is currently a lecturer and researcher in the Artificial Intelligence-Medical Center of Excellence, Universitas Sriwijaya, Palembang, Indonesia. Her research interests include biomedical signal/image processing, deep learning, and machine learning. She can be contacted at email: riset.annisadarmawahyuni@gmail.com or annisadarmawahyuni@unsri.ac.id.

Alexander Edo Tondas is currently a cardiologist in Department of Cardiology and Vascular Medicine, Dr. Mohammad Hoesin Hospital, Palembang. He can be contacted at email: tondas2000@gmail.com.

Muhammad Naufal Rachmatullah is currently a lecturer and researcher in the Artificial Intelligence-Medical Center of Excellence, Universitas Sriwijaya, Palembang, Indonesia. He can be contacted at email: naufalrachmatullah@gmail.com.

Firdaus is currently a lecturer and researcher in the artificial intelligence-medical center of excellence, Universitas Sriwijaya, Palembang, Indonesia. He can be contacted at email: virdauz@gmail.com.

Ade Iriani Sapitri is currently a lecturer and researcher in the Artificial Intelligence-Medical Center of Excellence, Universitas Sriwijaya, Palembang, Indonesia. She can be contacted at email: adeirianisapitri13@gmail.com.

Anggun Islami is currently a lecturer and researcher in the artificial intelligence-medical center of excellence, Universitas Sriwijaya, Palembang, Indonesia. She can be contacted at email: anggunislami2@gmail.com.

Sukemi is currently a lecturer and researcher in Department of Computer System, Faculty of Computer Science, Universitas Sriwijaya, Palembang, Indonesia. He can be contacted at email: sukemi@unsri.ac.id.

Muhammad Fachrurrozi is currently a lecturer and researcher in Department of Informatics Engineering, Faculty of Computer Science, Universitas Sriwijaya, Palembang, Indonesia. He can be contacted at email: obetsobets@gmail.com.

Siti Nurmaini is currently a professor and researcher in the Artificial Intelligence-Medical Center of Excellence, Universitas Sriwijaya, Palembang, Indonesia. She received her Master's degree in Control Systems from Institut Teknologi Bandung (ITB), Indonesia, in 1998, and her Ph.D. degree in Computer Science from Universiti Teknologi Malaysia (UTM) in 2011. Her research interests include biomedical engineering, deep learning, machine learning, image processing, control systems, and robotics. She can be contacted at email: sitinurmaini@gmail.com.

Rendy Isdwanta is currently alumni at Faculty of Computer Science, Universitas Sriwijaya, Indonesia. His research interest includes machine learning, signal/image processing, and deep learning. He can be contacted at email: risdwanta@gmail.com.

Jordan Marcelino is currently alumni at Faculty of Computer Science, Universitas Sriwijaya, Indonesia. His research interest includes machine learning, signal/image processing, and deep learning. He can be contacted at email: jhordan.marcelino@gmail.com.